arXiv:cond-mat/0405568v1 [cond-mat.mes-hall] 24 May 2004

Transport in single-molecule transistors: Kondo physics and negative differential resistance

Lam H. Yu and Douglas Natelson

Department of Physics and Astronomy, Rice University, 6100 Main St., Houston, TX 77005

Abstract. We report two examples of transport phenomena based on sharp features in the effective density of states of molecular-scale transistors: Kondo physics in C_{60}-based devices, and gate-modulated negative differential resistance (NDR) in "control" devices that we ascribe to adsorbed contamination. We discuss the need for a statistical approach to device characterization, and the criteria that must be satisfied to infer that transport is based on single molecules. We describe apparent Kondo physics in C_{60}-based single-molecule transistors (SMTs), including signatures of molecular vibrations in the Kondo regime. Finally, we report gate-modulated NDR in devices made without intentional molecular components, and discuss possible origins of this property.

E-mail: natelson@rice.edu

PACS numbers: 72.80.Rj,73.63.Rt,73.23.Hk

1. Introduction

Though active electronic devices made from molecules were originally suggested thirty years ago[1], interfacing small numbers of molecules with metal electrodes for electronic characterization has only been successful relatively recently[2, 3]. Two-terminal configurations include nanopore[4] structures[5, 6], crossed wires [7, 8, 9], mechanical break junctions[10, 11, 12, 13, 14], and scanned probe approaches (scanning tunneling microscope (STM)[15, 16, 17, 18, 19, 20] or conducting probe atomic force microscope (AFM)[21, 22]).

The resulting two-terminal devices exhibit a number of interesting phenomena, including molecular rectification[23], negative differential resistance (NDR)[5], and switching between low and high conductance states[7, 8, 6, 19, 20]. Several explanations for these effects have been proposed, including: the electronic structure of the molecular orbitals[24, 25]; conformational changes in the molecules[26, 24, 27, 28, 29]; vibronic-assisted inelastic tunneling[30, 31, 32]; and dynamic switching of contact bonds[20]. A central question is whether the nonlinear effects are intrinsic to the molecules themselves, or the molecule-metal contact. *Three-terminal* devices provide added tunability to test candidate explanations for nonlinear conduction in these systems.

Three-terminal nanometer-scale single molecule transistors (SMTs)[33, 34, 35, 36, 37, 38, 39] are a rich physical system, sensitive to molecular vibrational modes[33] and exhibiting correlated many-body states (the Kondo effect)[34, 35, 38]. Such devices are tools for examining physics on the nanometer scale, and promise to be the ultimate limit of electronic device scaling.

In this paper we report two different nonlinear conductance phenomena in molecule-scale three-terminal devices. First, we show conduction in C_{60}-based single-molecule transistors consistent with Kondo physics. The data indicate that inelastic couplings to vibrational resonances in the molecule lead to enhanced transport at finite bias in the Kondo regime. We also show that nanometer-scale metal junctions can, under certain circumstances, exhibit pronounced negative differential resistance tunable by a proximal gate electrode. We argue that this NDR most probably originates from the adsorption of a specific contaminant at the nanometer-scale interelectrode gap.

2. Technique

Devices are prepared on an oxidized (200 nm), degenerately doped $p+$ Si substrate that is used as an underlying gate electrode. The fabrication technique, based on controlled electromigration of lithographically fabricated metal constrictions[40], is shown in Fig. 1 and described in further detail in Ref. [38]. A Ti (1.5 nm)/Au (15 nm) metal constriction between two larger pads made by electron beam lithography, e-beam evaporation, and lift-off. The surface is then exposed to oxygen plasma for 1 min. to remove any organic residue from the lithography process. Batches of as many as 60 constrictions are fabricated on a single chip. The transverse dimension of the narrowest portion of

the constriction is typically 80 nm.

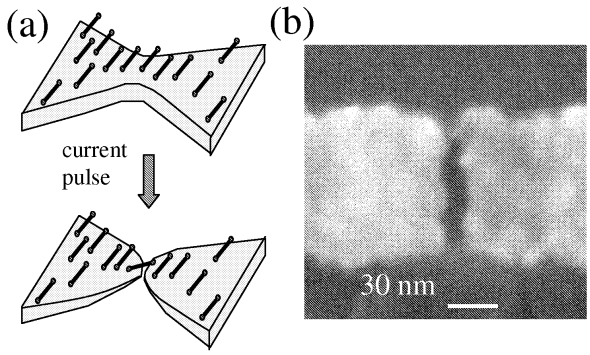

Figure 1. (a) Diagram of electromigration technique for fabrication of closely spaced electrodes bridged by individual molecules. (b) Micrograph of typical result, with electrodes separated by < 3 nm.

For C_{60}-based devices, a dilute solution (1 mg C_{60}/ 4 mL toluene) of molecules is spin cast (900 rpm) onto the array of constrictions. The wafer is then placed in a variable-temperature vacuum probe station that is evacuated to $<\sim 10^{-5}$ mB by turbopump. Control devices are treated similarly, but without the fullerenes. Various common solvents have been examined, including toluene, tetrahydrofuran (THF), and methyl chloride. No particular precautions have been taken to avoid exposure to ambient atmosphere during the spinning process.

At room temperature a semiconductor parameter analyzer is used to sweep an applied voltage across the junction until the junction conductance begins to degrade from electromigration. This "prebreaking" is stopped once the junction resistance exceeds a few hundred Ohms. Subsequent examination of such junctions by scanning electron microscope (SEM) indicates that the junctions are nearly broken, so that the applied voltage drops almost entirely across the now nano-scale constriction.

The sample area is then cooled to 4.2 K by flowing liquid cryogens, while the chamber is isolated from the turbo pumping system. By carefully heating the sample stage during this cooling process, stray gases are cryoadsorbed to the chamber walls and a carbon felt "'sorb" rather than onto the sample. Cryopumping creates ultrahigh vacuum (UHV) conditions at the sample while at low temperatures. Further electromigration is performed at 4.2 K, breaking the constrictions into separate source and drain electrodes while in UHV.

Figure 1b shows an SEM image of such an electrode pair after warming to room temperature. From all the constrictions that begin intact at room temperature, measurable conduction at a source-drain bias of 100 mV is found at the conclusion of the electromigration procedure for 70% of devices. Because metal surfaces anneal and reconstruct upon warming, it is difficult to perform precise measurements of electrode morphology. However, it appears that electrodes must be spaced by 1-3 nm for measurable conduction.

All measurements reported here were performed at dc using a semiconductor parameter analyzer. For each electrode pair, one electrode (source) is defined as ground,

and $I_{\rm D}$ is measured as a function of $V_{\rm D}$ for various values of gate voltage, $V_{\rm G}$. Differential conductance, $dI_{\rm D}/dV_{\rm D}$, is then computed numerically. While numerical differentiation can be noisy, this procedure has the benefit of working over a very broad range of conductances.

In experiments done on the C_{60}-decorated junctions, the devices are usually thermal cycled once over a period of two days without venting the chamber. In the NDR experiments discussed below, electrodes were thermally cycled several times over three to five days. Device characteristics measured at low temperatures varied after each thermal cycle, presumably due to electrode surface reconstruction, molecule migration, and possible adsorption of contaminants such as water.

3. Device physics

3.1. Single-electron devices

All successful nanometer-scale single-molecule transistors that have been demonstrated[33, 34, 35, 36, 37, 38, 39] act as single-electron transistors (SETs)[41]. A SET consists of an island coupled by tunnel barriers ($R > R_{\rm K} \equiv h/e^2$) to source and drain electrodes, with additional capacitive coupling to a gate electrode. Accounting for electron-electron interactions on the island via a classical capacitance, one may define an electron addition energy, $E_{\rm c}$, associated with changing the charge of the island by a single electron. For $k_{\rm B}T << E_{\rm c}$, it is energetically forbidden at zero source-drain bias to change the charge state of the island. The resulting suppression of transport is Coulomb blockade. Higher order processes (*e.g.* cotunneling) can allow transport in the classically blockaded regime.

It is possible to use $V_{\rm G}$ to lift the blockade at zero source-drain bias by adjusting the potential of the island so that it is energetically degenerate to change the charge of the island by one electron. Similarly, current may flow once $eV_{\rm D}$ exceeds the energy addition threshhold. Mapping differential conductance as a function of $V_{\rm D}$ and $V_{\rm G}$, one finds a result like that shown in Fig. 2: diamond-shaped blockaded regions where the charge on the island is quantized, separated by a "crossing point" where, at $V_{\rm D} = 0$ and with increasing $V_{\rm G}$, the occupation of the island changes from n to $n+1$ electrons. The lower the capacitive coupling to the gate relative to the source and drain couplings, the more change in $V_{\rm G}$ necessary to change the charge state of the island.

For a small island $E_{\rm c}$ includes both the Coulomb repulsion, U_i, and the spacing between the ith and $i+1$th single-particle electronic states, Δ_i. When inelastic processes are allowed, at sufficient bias an electron may tunnel from the source into *excited* single-particle states of the island, as well as the lowest available single-particle state. Transport at high bias is enhanced by these additional channels, manifested as peaks in the differential conductance that parallel the edges of the blockaded diamonds.

When the island is a nanoscale molecule, several issues arise. First, source and drain couplings are established by overlap of the molecular wavefunction with that

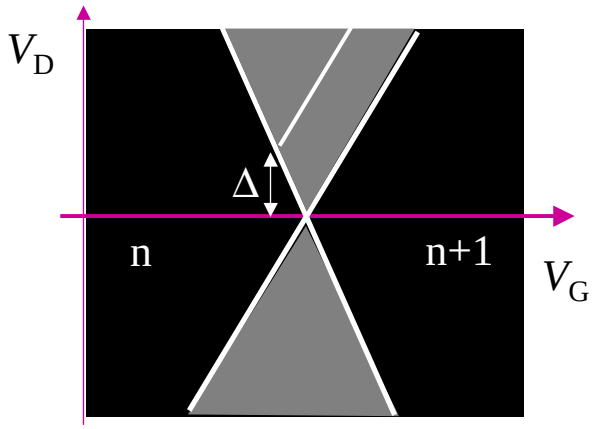

Figure 2. (a) Schematic map of differential source-drain conductance of asingle-electron transistor as a function of bias and gate voltage. Brightness scale runs from zero conductance (black) to high conductance (white). Arrow indicates a resonance due to tunneling into an excited state with energy Δ above the lowest unoccupied island state.

of the conduction electrons of the leads. These couplings broaden the energies of the single-particle states by Γ_S, Γ_D, and depend crucially on the details of the metal surface, the molecular orientation, and the chemical nature of the molecular binding. Furthermore, the classical capacitance is so small that electrostatic charging energies in excess of 100 meV are reasonable. Similarly, the spacings between the single-particle molecular states can easily be hundreds of meV or more. While there is some evidence that significant renormalizations of both these quantities may occur[37], most experiments[33, 34, 35, 36, 38] find accessing more than two charge states of a single molecule to be extremely challenging.

Because of these large level spacings, tunneling through excited electronic states is generally not seen in SMTs. However, molecules do exhibit vibrational excitations at the meV scale. Observations of tunneling through such excited states have been reported[33, 34, 35, 36, 38], as have vibrational effects in other gated molecular devices[42].

A single-electron device with an unpaired spin may demonstrate nontrivial transport physics[43, 44] due to the Kondo effect[45], the formation of a many-body state comprising the unpaired spin and an antiferromagnetically coupled screening cloud of conduction electrons in the leads. The energy scale, $k_B T_K$, for the Kondo effect depends exponentially on the total coupling $\Gamma = \Gamma_S + \Gamma_D$. It is possible to have a high Kondo temperature while still having a low total conductance, since the conductance is limited by the smaller of Γ_D, Γ_S while T_K is set by their total.

The signature of a Kondo resonance in a single-electron device is the appearance of a peak in the differential conductance near zero source-drain bias when the number of charges on the island changes from even to odd. In a well-coupled system for $T << T_K$ the peak conductance on resonance is expected to saturate to $2e^2/h$. This value may be significantly reduced if the source and drain couplings are very asymmetric.

For $T >\sim T_K$, the peak conductance is expected to decrease logarithmically with temperature. The shape of this resonance (I_D as a function of V_D) may deviate from a pure Lorentzian due to Fano-type competition between Kondo resonant transport and other channels[46, 47, 48]. In an external magnetic field, B, large enough to Zeeman split the localized, unpaired spin, the Kondo peak is expected to split by an amount $g\mu_B B$, where μ_B is the Bohr magneton and g is the Landé factor. Kondo physics has been reported in molecular devices incorporating metal ions[34, 35]. Our observation of C_{60}-based devices is described below. We discuss vibrational resonances in the Kondo regime, a phenomenon only observable in molecular devices.

3.2. Negative differential resistance

Negative differential resistance is well known and understood in two-terminal devices such as $p-n$ junctions[49], quantum well resonant tunneling diodes[50], and scanning tunneling spectroscopy (STS) measurements[51]. The basic mechanism for each involves energy-specific conduction of charge carriers; as the source-drain bias is swept into and out of the relevant energy range, the current varies nonmonotonically, leading to NDR over some range of bias voltage. In Esaki diodes the current peaks due to the alignment of the valence and conduction bands across the $p-n$ junction over a limited range of bias. In quantum well devices the increase in conduction occurs when the energy of the injected carriers is resonant with a quasi-bound state of the well. Here we will explore the origin of NDR in the STS measurements[52] in more detail because we believe a similar mechanism is responsible for our NDR observations.

Consider a tunneling spectroscopy measurement with electrons flowing from a probe tip to a conducting substrate, with a molecule attached to the substrate. To explain the observation of NDR one must abandon the common notion of a featureless tip density of states, and describe the current through the STS system with the general expression:

$$I = \int_{\mu_S}^{\mu_P} T(E,V)dE, \tag{1}$$

where μ_S and μ_P are the electrochemical potential of the metallic substrate and probe tip, respectively, with $\mu_S = \mu_P + eV$. Here $T(E,V)$ is the tunneling transmission of the system. Using the transfer Hamiltonian formalism, one can relate $T(E,V)$ to the product of the local densities of states (LDOS) $\rho_{mol}(E)$ and $\rho_{tip}(E)$ of the molecule and the tip. The current through the STS system is proportional to the convolution of ρ_{mol} and ρ_{tip} within the energy range defined by μ_S and μ_P.

Suppose both the ρ_{mol} and the ρ_{tip} contain sharp peaks (such as those caused by localized surface states, for example[53]). As the bias is applied the LDOS shift relative to one another, and it is possible for the energies of the sharp features to become commensurate. If this alignment happens when one sharp feature is occupied and the other is empty, one may observe NDR. This situation is illustrated in Figure 3b,c,e. As the LDOS peaks move toward (away from) each other in energy while the bias is swept, the current will increase (decrease).

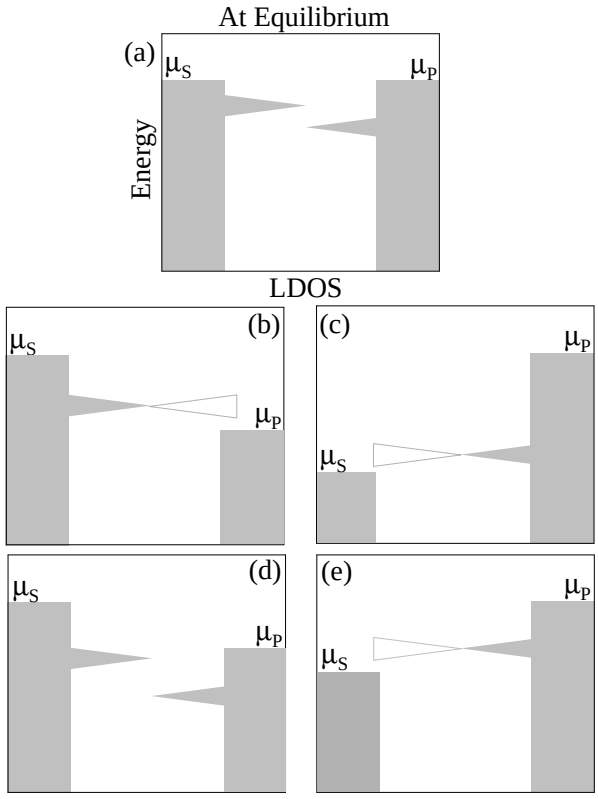

Figure 3. Energetics of substrate/molecule and tip apex/probe in STS measurements on molecules, after [52]. Sharp features represent local densities of states of the molecule (left) and the tip apex (right). Weak coupling allows a potential difference to develop between the molecule and substrate under bias. (a) At equilibrium, with substrate chemical potential, μ_S, and probe chemical potential, μ_P; (b) A positive bias V is applied to the probe, and weak apex-probe coupling is assumed, leading to the apex potential $V_{\rm Apex} < V$. The LDOS of the apex atom moves up relative to μ_P under bias, and NDR results; (c) A negative bias is applied to the probe, again with $|V_{\rm Apex}| < |V|$. The LDOS of the apex atom move down relative to μ_P, and NDR results; (d) A positive bias is applied to the probe, with strong apex-probe coupling that forces $V_{\rm Apex} = V$. No NDR results because of relative positions of molecule and apex LDOS (e) A negative bias is applied to the probe, with $V_{\rm Apex} = V$. Since the LDOS of the molecule must move down with respect to the μ_P under bias, NDR results.

It is important to consider whether one expects to find NDR under both signs of bias within this picture; both cases are observed in STS. As explained in Ref. [52], the critical issue is whether there is significant voltage dropped between the apex of the probe tip (source of the sharp LDOS peak) and the bulk of the probe tip (and similarly between the molecule and the substrate). If the apex and bulk of the tip are essentially at the same chemical potential, then NDR is only expected under one bias direction (Figure 3d,e). Note that a weak coupling between the apex and bulk of the tip, a necessary condition for the observation of NDR under both signs of bias, would also imply poor screening near the tip apex. This is relevant when considering the effects of a proximal gate electrode.

4. Device characterization and statistics

At present no microscopy technique allows direct assessment of the presence of a single nanometer-scale molecule at the source-drain interelectrode gap. Therefore one must infer such information from transport measurements and control experiments. Every electrode pair produced by the electromigration process is different at the nanometer scale. Similarly, the positions, orientations, couplings to source, drain, and gate electrodes, of possible molecules near the interelectrode gaps are all probabilistic. With this fabrication technique *a statistical approach with large numbers of devices is essential.*

Conduction characteristics at low temperatures after electromigration may be divided into four general classes:

A. *No detectable source-drain current.* The most likely explanation, confirmed by SEM observation, is that the resulting interelectrode gap is too large for detectable source-drain conduction by either tunneling, thermionic, or field emission.

B. *Weak nonlinearity, no gate response.* This is the result most commonly seen in bare metal control devices, and presumably corresponds to electrodes sufficiently close (1-2 nm) for some conduction, but without a molecule in the gap.

C. *Strong nonlinearity, no gate response.* The most probable explanation for such $I_{\rm D}-V_{\rm D}$ characteristics is that a molecule or metal nanoparticle is positioned between the source and drain, but device geometry results in extremely poor gate coupling.

D. *Strong nonlinearity, gate response.* These are the devices of interest, and consist of either a molecule, group of molecules, contaminant, or metal nanoparticle between nanometer-separated source and drain.

Table 1 shows the statistics of all 724 devices prepared using C_{60} molecules.

Table 1. Device yield statistics of C_{60} SMTs.

$I_{\rm D}-V_{\rm SD}$ curve type	Interpretation	% of devices
none	gap too large	30%
weakly nonlinear	no molecule	38%
strongly nonlinear, no gating	no gate coupling	19%
strongly nonlinear + gating	candidate SMT	13%

Given a gateable, nonlinear $I_{\rm D}-V_{\rm D}$ characteristic consistent with Coulomb blockade, it is *essential* to consider four other issues to help determine whether the device is a SMT or a result of metal nanoparticles produced in the electromigration process. First, is the electron addition energy (the maximum source-drain bias of the blockaded region) of a sensible size for the molecule under consideration? As mentioned above, the *minimum* addition energy, even in the absence of molecular level spacings, should be sensibly large for Coulomb charging of a nanoscale object in a dielectric

environment. Addition energies significantly less than 50 meV should be considered carefully.

Second, are the number of accessible charge states of the device reasonable for a molecule? Solution-based electrochemistry provides an upper limit to the number of valence states that one should reasonably be able to explore. In electrochemical experiments, the excess molecular charge is compensated by the presence of ions in the solvent that can be within a nanometer of the molecule. This screening should be more efficient than any possible in a conventional field effect geometry, even with an extremely thin gate dielectric. For example, C_{60} may be reduced in solution only a few times. Therefore if one finds that it is possible to add ten or twenty electrons to a candidate device via gating (*i.e.* there are many Coulomb blockade crossing points), it is extremely unlikely that the active region of the candidate device is a single C_{60} molecule. This issue makes interpretation of some data[39] challenging.

Third, are the particular gateable, nonlinear characteristics observed only when molecules are present? We have observed clear Coulomb blockade with various electron addition energies in a small percentage of bare metal control devices. Clearly Coulomb blockade characteristics alone are not sufficient to confirm the molecular character of a SMT. Similarly, the NDR effects described below appear predominantly in devices prepared *without* C_{60} molecules, and therefore cannot represent a property of C_{60}-based conduction.

Finally, are there features in the data that uniquely specify the molecule? Known vibrational resonances in particular can be extremely useful, and have been identified in several experiments[33, 36, 38].

5. Results and discussion

5.1. C_{60} devices and Kondo physics

Figure 4a is a conductance map of a C_{60}-based SMT measured at 5 K. Coulomb blockade is clearly evident, as is an uncontrolled change in offset charge (the discontinuity at $V_G = 8$ V). Note that the electron addition energy significantly exceeds 100 meV, and that there are vibrational resonance features at ~ 35 meV, as indicated by the arrows. Much of the noise in the data are an artifact of the numerical differentiation procedure. Scans out to higher gate voltages in both polarities revealed no further Coulomb blockade crossing points. This indicates that we were only able to change the charge state of this device by a single electron.

Figure 4b is a conductance map for a SMT that appears consistent with Kondo physics. At gate voltages less than -10 V, conductance is consistent with Coulomb blockade, including a likely vibrational resonance at ~ 35 meV. When V_G is swept past the charge degeneracy point, a pronounced peak appears at zero bias. Notice that the 35 meV peak continues into this regime. In fact both the 35 meV conductance and the zero-bias conductance are enhanced relative to the conductances measured in the

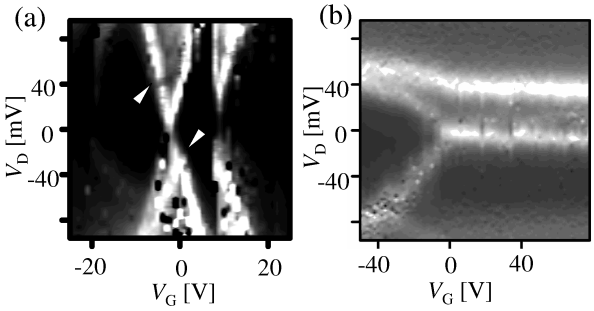

Figure 4. (a) Map of differential source-drain conductance of a C_{60}-based SMT at 5 K, as a function of bias and gate voltage. Brightness scale runs from zero conductance (black) to 3×10^{-6} S (white). Arrows indicate 35 meV resonances due to vibrational mode of C_{60}. (b) Analogous map for a device exhibiting conduction consistent with Kondo physics. Conductance range is from zero (black) to 1.5×10^{-5} S (white).

Coulomb blockade regime. Some indications of vibrational signatures in the Kondo regime were present in an earlier experiment[35]. In the C_{60} case shown here, however, the vibrational mode is known. We also note that enhanced coupling to vibrational modes in the presence of a strong coupling between adsorbed molecular charge and metal conduction electrons is known to occur in other cases, such as the "chemical enhancement" contribution to surface-enhanced Raman scattering[54].

A detailed analysis of several samples similar to that in Fig. 4b is presented in Ref. [38]. Several points are noteworthy. First, only ∼1-2% of C_{60}-decorated electrodes eventually resulted in devices that showed this Kondo-like conductance map. This is unsurprising when one recalls that T_K depends exponentially on Γ, which itself is exponentially sensitive to molecule-metal geometry. Similarly, presumably because of these steep dependences, we found it extremely difficult to perform characterization of such devices over a broad temperature range due to irreversible changes in device characteristics. Figure 5 shows an example of this instability. At left is the conductance map of the device showing the transition to having the zero-bias resonance. During an attempt to characterize the temperature dependence of the zero-bias peak, the device spontaneously changed to a different configuration. Subsequent measurements of the device yielded conductance characteristics like that shown in the plot at right, looking like Coulomb blockade with poor gate coupling. The typical maximum conductance remains $\sim 10^{-5}$ S despite this change in coupling, consistent with the idea that the couplings to the leads are asymmetric, as discussed above.

From the limited T-dependence data acquired, the zero-bias peak is essentially independent of T below $\sim$ 20 K. Within the Kondo picture the width of the peak is proportional to T_K when T is sufficiently below T_K. Our data are consistent with values of T_K of around 100 K or more. This energy scale is so large that resolving Zeeman splitting of the peak is unfeasible.

The high Kondo temperatures inferred in the C_{60} system may explain another observation[55] in scanning tunneling microscopy (STM) using probe tips made from C_{60} adsorbed on platinum-iridium. Those STM measurements indicated a surprisingly

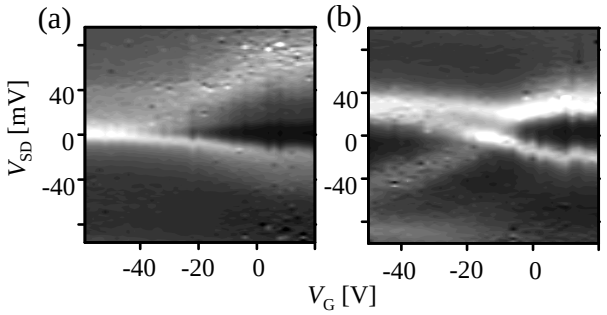

Figure 5. Example of an irreversible change from Kondo-like conduction (a) to conventional Coulomb blockade conduction (b) in a single device, likely due to an uncontrolled rearrangement of the molecule-electrode tip geometry. Conductance is from zero (black) to 1.8×10^{-5} S (white).

narrow, peaked density of states for the tips. One explanation for such a feature would be a Kondo resonance between the physisorbed C_{60} and the tip, perhaps surviving even at 300 K. Experiments on C_{60} SMTs with Pt electrodes are planned. We note that fabricating SMTs that are mechanically and electrically stable and exhibit Kondo physics at room temperature would have significant implications for practical devices. Such SMTs would be switchable by gating from a Coulomb blockaded state to resonant conduction with conductances approaching $2e^2/h$, the theoretical maximum per molecule. Such devices would remain vulnerable to offset charge problems characteristic of single-electron architectures[56]. They would, however, offer the only known means of modulating such high conductances per molecule apart from larger structures involving perfectly contacted carbon nanotubes.

5.2. Negative differential resistance

In a series of control experiments, electromigrated control samples that were exposed to various solvents (e.g. THF, toluene, methyl chloride) prior to being place in the vacuum probe station were thermally cycled multiple times over the course of three to five days. In 10% of 175 multiple thermal cycled control devices we observed regions of NDR in their $I_D - V_D$ curves at 4.2 K, such as those shown in Figure 6.

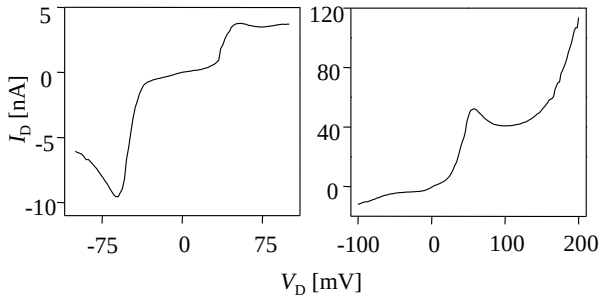

Figure 6. Examples of $I_D - V_D$ characteristics ($V_G = 0$, $T = 4.2$ K) for control samples (no C_{60}) exposed to non-UHV conditions repeatedly. NDR can occur for either one or both bias polarities.

We suggest that the NDR results from sharp features in the densities of states of the source and drain electrodes due to adsorbed impurities. The role of unintended adsorbates seems clear, since the NDR tends to appear as surfaces are exposed for significant periods in non-UHV conditions. We believe that there is *one particular kind of adsorbate* that causes the NDR in our control devices. The evidence for our assertion is shown in Fig. 7, a histogram of the bias position (at zero gate voltage) where the maximum NDR occurs for these devices. The histogram is peaked prominently near 75 mV, suggesting that the NDR in these devices has a well-defined, common origin, rather than being a random phenomenon.

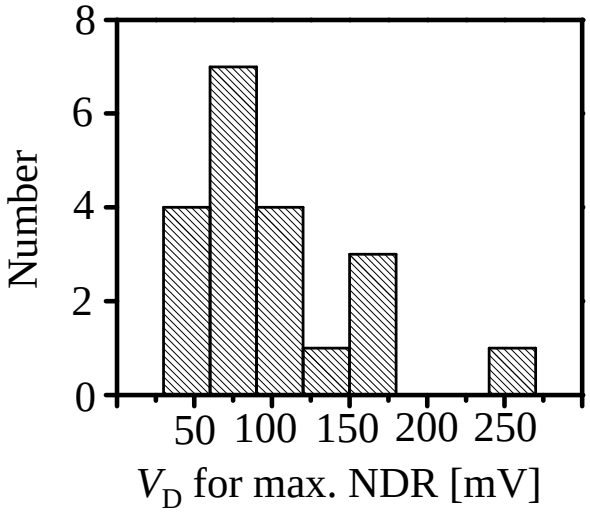

Figure 7. For $V_G = 0$, distribution of bias voltages at which maximum NDR occurs. The histogram is singly peaked, suggesting that a single specific mechanism is producing the NDR effect.

Similar to STS experiments where NDR were observed[51, 52], we also observe in these devices that NDR can appear in either only one or both bias directions. About 30% of the NDR devices exhibit NDR in both bias polarities. All devices that exhibit NDR in both bias directions are also gateable. The conductance map of such a device is shown in Figure 8. Regions of NDR are indicated by the arrows.

The concurrency of NDR in both bias directions and the gateablity of the devices reflects the extended screening length in the metal-molecule junction when the apex of the electrode is weakly coupled to the bulk of the electrode. If the screening length is long enough for the emergence of a voltage drop between the apex and the bulk of the electrode, then it would likely to be long enough for the gate to influence the electrostatic potential of the metal-molecule junction.

The fact that the nonlinear conduction can be modulated by V_G even in the absence of Coulomb blockade strongly constrains alternative NDR explanations. For example, vibrationally mediated NDR sometimes observed in STS experiments on adsorbed molecules[30] is only expected to occur at biases that correspond to specific mechanical modes of the adsorbate. Since those vibrational modes are determined by molecular structure rather than electrostatics, gate-independent NDR would be expected from

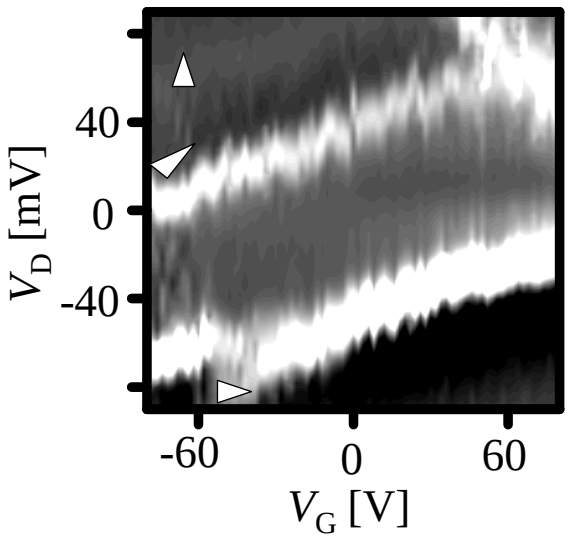

Figure 8. Differential conductance map of a control device showing gateable NDR. Brightness runs from -8×10^{-8} S (black) to 2×10^{-7} S (white). Arrows indicate NDR regions.

this mechanism. Similarly, the lack of correlation of NDR with Coulomb charging implies that the molecular orbital effects suggested[24] to explain some nanopore NDR observations[5] are not relevant.

Experiments are ongoing to determine the particular adsorbates responsible for the NDR. As with the Kondo physics discussed above, a reliable method to create stable, nanometer-scale NDR devices with significant peak-to-valley ratios would have significant practical implications.

6. Summary

We have employed an electromigration technique to create three terminal devices with source and drain electrodes separated on the single nanometer scale. With these devices we have demonstrated single-molecule transistors based on C_{60} that operate as single-electron devices that can access two molecular charge states. Some of these C_{60} SMTs exhibit conductance properties consistent with Kondo physics. Kondo transport here is indicated by the presence of a zero-bias peak in the conductance for one SMT charge state, and Coulomb blockade for the other. The role of C_{60} is indicated by resonance features in the conductance energetically compatible with known molecular vibrational modes. Because of the resonant nature of conduction in the Kondo regime, this physics holds out the promise of SMTs with a conductance per molecule in the "on" state approaching the theoretical maximum, $2e^2/h$.

Control devices left exposed to non-UHV conditions demonstrate a propensity to exhibit negative differential resistance. We have shown that this NDR may be modulated via V_G, and propose that its explanation lies in sharp peaks in the local densities of states of the source and drain electrodes due to adsorbed impurities. We argue that the

peaked distribution of NDR voltage characteristics implies that a single type of impurity is responsible for this nonlinear conduction. An improved understanding of this system may allow the controlled engineering of molecule-scale NDR devices.

Acknowledgments

The authors thank K. Kelly and A. Osgood for STM characterization, and P.L. McEuen, P. Nordlander, H. Park, D.C. Ralph, A. Rimberg, J.M. Tour, and R.L. Willett for useful conversations.

This work was supported by the Robert A. Welch Foundation, the Research Corporation, the David and Lucille Packard Foundation, and the National Science Foundation.

[1] Aviram A and Ratner M 1974 *Chem. Phys. Lett.* **29** 277–283
[2] Nitzan A and Ratner M 2003 *Science* **300** 1384–1389
[3] Tour J 2000 *Acc. Chem. Res.* **33** 791–804
[4] Ralls K and Buhrman R 1988 *Phys. Rev. Lett.* **60** 2434–2438
[5] Chen J, Reed M A, Rawlett A M and Tour J M 1999 *Science* **286** 1550
[6] Reed M A, Chen J, Rawlett A M, Price D W and Tour J M 2001 *Appl. Phys. Lett.* **78** 3735–3737
[7] Collier C, Wong E, Belohradsky M, Raymo F, Stoddart J, Keukes P, Williams R and Heath J 1999 *Science* **285** 391–394
[8] Collier C, Mattersteig G, Wong E, Luo Y, Beverly K, Sampaio J, Raymo F, Stoddart J and Heath J 2000 *Science* **289** 1172–1175
[9] Kushmerick J, Holt D, Yang J, Naciri J, Moore M and Shashidar R 2002 *Phys. Rev. Lett.* **89** 086802
[10] van Ruitenbeek J, Alvarez A, Piñeyro I, Grahmann C, Joyez P, Devoret M, Esteve D and Urbina C 1996 *Rev. Sci. Instr.* **67** 108–111
[11] Reed M, Zhou C, Muller C, Burgin T and Tour J 1997 *Science* **278** 252–254
[12] Scheer E, Agraït N, Cuevas J C, Yeyati A L, Ludolph B, Martin-Rodero A, Bollinger G R, van Ruitenbeek J M and Urbina C 1998 *Nature* **394** 154–157
[13] Reichert J, Ochs R, Beckmann D, Weber H, Mayor M and von Lohneysen H 2002 *Phys. Rev. Lett.* **88** 176804
[14] Smit R, Noat Y, Untiedt C, Lang N, van Hemert M and van Ruitenbeek J 2002 *Nature* **419** 906–909
[15] Joachim C, Gimzewski J, Schlittler R and Chavy C 1995 *Phys. Rev. Lett.* **74** 2102–2105
[16] Yazdani A, Eigler D and Lang N 1996 *Science* **272** 1921–1924
[17] Datta S, Tian W, Hong S, Reifenberger R, Henderson J I and Kubiak C P 1997 *Phys. Rev. Lett.* **79** 2530–2533
[18] Stipe B, Rezaei M and Ho W 1998 *Science* **280** 1732–1735
[19] Donhauser Z J, Mantooth B A, Kelly K F, Bumm L A, Monnell J D, Stapleton J J, Jr D W P, Rawlett A M, Allara D K, Tour J M and Weiss P S 2001 *Science* **292** 2303–2307
[20] Ramachandran G, Hopson T, Rawlett A, Nagahara L, Primak A and Lindsay S 2003 *Science* **300** 1413–1416
[21] Wold D and Frisbie C 2001 *J. Am. Chem. Soc.* **123** 5549–5556
[22] Cui X D, Primak A, Zarate X, Tomfohr J, Sankey O F, Moore A L, Moore T A, Gust D, Harris G and Lindsay S M 2001 *Science* **294** 571–574
[23] Metzger R, Chen B, Höpfner U, Lakshmikantham M, Vuillaume D, Kawai T, Wu X, Tachibana H, Hughes T, Sakurai H, Baldwin J, Hosch C, Cava M, Brehmer L and Ashwell G 1997 *J. Am. Chem. Soc.* **119** 10455–10466
[24] Seminario J, Zacarias A and Tour J 2000 *J. Am. Chem. Soc.* **122** 3015–3020

[25] Seminario J, Zacarias A and Derosa P 2001 *J. Phys. Chem. A* **105** 791–795
[26] Seminario J, Zacarias A and Tour J 1998 *J. Am. Chem. Soc.* **120** 3970–3974
[27] Emberly E and Kirczenow G 2001 *Phys. Rev. B* **64** 125318
[28] Solak A, Ranganathan S, Itoh T and McCreery R 2002 *Elect. Sol. State Lett.* **5** E43–E46
[29] Troisi A and Ratner M 2002 *J. Am. Chem. Soc.* **124** 14528–14529
[30] Gaudioso J, Lauhon L and Ho W 2000 *Phys. Rev. Lett.* **85** 1918–1921
[31] Kuznetsov A and Ulstrup J 2002 *J. Chem. Phys.* **116** 2149–2165
[32] Troisi A, Ratner M and Nitzan A 2003 *J. Chem. Phys.* **118** 6072–6082
[33] Park H, Park J, Lim A, Anderson E, Alivisatos A and McEuen P 2000 *Nature* **407** 57–60
[34] Park J, Pasupathy A N, Goldsmith J I, Chang C, Yaish Y, Petta J R, Rinkowski M, Sethna J P, Abruña H D, McEuen P L and Ralph D C 2002 *Nature* **417** 722–725
[35] Liang W, Shores M P, Bockrath M, Long J R and Park H 2002 *Nature* **417** 725–729
[36] Park J, Pasupathy A, Goldsmith J, Soldatov A, Chang C, Yaish Y, Sethna J, Abruña H, Ralph D and McEuen P 2003 *Thin Solid Films* **438-439** 457–461
[37] Kubatkin S, Danilov A, Hjort M, Cornil J, Brédas J L, Stuhr-Hansen N, Hedegård P and Bjornholm T 2003 *Nature* **425** 698–701
[38] Yu L H and Natelson D 2004 *Nano Letters* **4** 79–83
[39] Yu H, Luo Y, Beverly K, Stoddart J, Tseng H R and Heath J 2003 *Angew. Chem. Int. Ed.* **42** 5706–5711
[40] Park H, Lim A K L, Alivisatos A P, Park J and McEuen P L 1999 *Appl. Phys. Lett.* **75** 301–303
[41] Grabert H and Devoret M H, editors 1992 *Single Charge Tunneling: Coulomb Blockade Phenomena in Nanostructures* NATO ASI series B: Physics Vol. 294 (New York: Plenum)
[42] Zhitenev N B, Meng H and Bao Z 2002 *Phys. Rev. Lett.* **88** 226801
[43] Goldhaber-Gordon D, Shtrikman H, Mahalu D, Abusch-Magder D, Meirav U and Kastner M 1998 *Nature* **391** 156–159
[44] Cronenwett S, Oosterkamp T and Kouwenhoven L 1998 *Nature* **281** 540–544
[45] Kondo J 1964 *Prog. Theor. Phys.* **32** 37–49
[46] Madhavan V, Chen W, Jamneala T, Crommie M and Wingreen N 1998 *Science* **280** 567–569
[47] —— 2001 *Phys. Rev. B* **64** 165412–1–165412–11
[48] Göres J, Goldhaber-Gordon D, Heemeyer S, Kastner M, Shtrikman H, Mahalu D and Meirav U 2000 *Phys. Rev. B* **62** 2188–2194
[49] Esaki L 1958 *Phys. Rev.* **109** 603–604
[50] Sollner T, Goodhue W, Tannenwald P, Parker C and Peck D 1983 *Appl. Phys. Lett.* **43** 588–590
[51] Lyo I and Avouris P 1989 *Science* **243** 1369–1371
[52] Xue Y, Datta S, Hong S, Reifenberger R, Henderson J and Kubiak C 1999 *Phys. Rev. B* **59** R7852–R7855
[53] Lang N 1997 *Phys. Rev. B* **55** 9364–9366
[54] Moskovits M, Tay L L, Yang J and Haslett T 2002 *Top. Appl. Phys.* **82** 215–227
[55] Kelly K, Sarkar D, Hale G, Oldenburg S and Halas N 1996 *Science* **273** 1371–1373
[56] Likharev K 1999 *Proc. IEEE* **87** 606–632